Available online at www.sciencedirect.com
SCIENCE DIRECT®
Nonlinear Analysis: Real World Applications 7 (2006) 432–457
Nonlinear Analysis
Real World Applications
www.elsevier.com/locate/na

Non-linear characteristics of a membrane fermentor for ethanol production and their implications

Andrés Mahecha-Botero[a,*], Parag Garhyan[b], S.S.E.H. Elnashaie[b]

[a] *Universidad Pontificia Bolivariana, Facultad de Ingeniería Química, Medellín, Colombia*
[b] *Chemical Engineering Department, Auburn University, Auburn, AL 36849, USA*

Received 29 June 2004; accepted 28 March 2005

Abstract

An experimentally verified five-dimensional model for anaerobic fermentation is used to explore the complex non-linear behaviour of a continuous membrane fermentor. Detailed modeling and detailed static/dynamic investigation are carried out with special emphasis on static/dynamic bifurcation and the effect of selective ethanol removal. Possible increase of sugar conversion and ethanol yield/productivity under autonomous periodic operation at high sugar concentrations was found for continuous stirred tank fermentors with/without ethanol removal membranes. The investigation shows that the ethanol selective membrane does not act only as an ethanol production enhancer but also as a stabilizer for the unstable fermentor. The present paper covers a wide range of parameters showing the non-linear richness of the process and the implication of the complex non-linear steady state and dynamic characteristics on the process ethanol yield and productivity.

Keywords: Modelling; Dynamic simulation; Nonlinear dynamics; Nonlinear analysis; Bifurcation; Fermentation; Product inhibition; Ethanol production

* Corresponding author. Chemical and Biological Engineering Department, The University of the British Columbia (U.B.C.), 2216 Main Mall, Vancouver, BC, Canada V6T-1Z4. Tel.: +1 604 822 3457; fax: +1 604 822 6003.
E-mail address: andresm@chml.ubc.ca (A. Mahecha-Botero).

1468-1218/$ - see front matter © 2005 Elsevier Ltd. All rights reserved.
doi:10.1016/j.nonrwa.2005.03.010

Nomenclature

C_i	Concentration of component i (kg/m^3)
$\overline{C_i}$	Average concentration of component i (kg/m^3)
r_i	Production rate of component i (kg/m^3 h)
C_{S_0}	Inlet substrate concentration (kg/m^3)
$D_{M_{in}}$	Inlet membrane dilution rate, inlet flow rate/membrane volume (h^{-1})
$D_{M_{out}}$	Output membrane dilution rate, output flow rate/membrane volume (h^{-1})
D_{in}	Inlet fermentor dilution rate, inlet flow rate/for monitor volume (h^{-1})
D_{out}	Output fermentor dilution rate, output flow rate/fermentor volume (h^{-1})
A_M	Area of membrane (m^2)
X_S	Substrate conversion
$\overline{X_S}$	Average substrate conversion
Y_P	Combined product yield from the fermentor and membrane (ethanol)
$\overline{Y_P}$	Combined average product yield from the fermentor and membrane (ethanol)
P_P	Combined production rate from the fermentor and membrane (g/h)
$\overline{P_P}$	Combined average production rate from the fermentor and membrane (g/h)
R_{ER}	Rate of membrane ethanol removal (g/h)
$\overline{R_{ER}}$	Average rate of membrane ethanol removal (g/h)
K_S	Monod constant (kg/m^3)
k_1	Empirical constant (h^{-1})
k_2	Empirical constant (m^3/kg h)
k_3	Empirical constant (m^6/kg^2 h)
m_s	Maintenance factor based on substrate (kg/kg h)
m_p	Maintenance factor based on product (kg/kg h)
Y_{sx}	Yield factor based on substrate (kg/kg)
Y_{px}	Yield factor based on product (kg/kg)
V_M	Membrane volume (m^3)
V_F	Fermentor volume (m^3)
P	Membrane permeability (m/h)

Greek symbols

ρ	Ethanol density (kg/m^3)
μ	Specific growth rate (hr^{-1})
τ	Period of oscillation (hr)

Subscripts i

S	Substrate (glucose) inside the fermentor
S_0	Influent glucose to the fermentor
P	Product (ethanol) inside the fermentor

P_0	Influent ethanol to the fermentor
e	Internal key component inside the fermentor
e_0	Influent internal key component to the fermentor
X	Biomass (microorganisms) inside the fermentor
X_0	Influent biomass to the fermentor
P_m	Product (ethanol) inside the membrane
P_{m_0}	Influent ethanol to the membrane

1. Introduction

Ethanol derived from renewable sources such as lignocellulosic wastes/materials is an attractive clean fuel to control air pollution and reduce the dependence on fossil fuels [23,28]. Ethanol is one of the most promising alternative fuels, either as fuel-ethanol or for blending with gasoline [1]. More recently, it has been also used as an oxygenate for the control of automotive tailpipe emissions [15,22,30]. Due to high feedstock prices for production of ethanol and competition from other products for its gasoline uses, it is necessary to make the process of ethanol production more efficient and economical. In this paper, we integrate nonlinear dynamics tools with membranes science (i.e. using a permselective membrane to remove product ethanol) to enhance the production of ethanol in continuous stirred tank fermentors.

The present investigation is an extension of the previous work by the authors regarding ethanol producing membrane fermentors [12,13]. In this paper, it is shown that operating the system at periodic states gives higher ethanol productivity/yield and sugar conversion as compared to the operation at the corresponding steady states. Furthermore, the effect of introducing an ethanol selective membrane is investigated and new phenomena discovered. It is shown that the ethanol removal membrane acts as a stabilizer for the fermentor.

2. Fundamentals

2.1. The biocatalyzing microorganism

Zymomonas mobilis has been promoted as a more promising microorganism than yeast for the industrial production of ethanol [24]. Continuous fermentation using *Zymomonas mobilis* has the incidence of oscillatory behaviour in which biomass, product and substrate cycle under certain fermentation conditions [5,12,13,16,24]. An experimental fermentor has been modeled by Jobses et al. [18–20]. This same model has been used by Al-Haddad [2] and Garhyan et al. [12] to uncover static and dynamic bifurcations as well as chaos. Their work used a four-dimensional model for anaerobic fermentation with *Zymomonas mobilis* in a continuous stirred tank fermentor at high glucose feed concentrations.

2.2. Product inhibition

Ethanol production by *Zymomonas mobilis* is, like most anaerobic fermentations [3], subject to end-product inhibition [18–20]. The product alters the cell membrane composition and inhibits enzymatic reactions [1] like carrier-mediated transport processes and metabolic conversion syntheses [20]. In this work, we are investigating the phenomena associated with the use of an ethanol removal membrane, in order to avoid ethanol inhibition in the fermentation process.

If ethanol could be removed as it is being produced, inhibition would be prevented. Cell activity would be maintained at high level, a higher glucose feed concentration could be used, and fermentor cell density will be increased [6,9,25]. The increased cell activity and cell density will keep volumetric productivity at high level, thus requiring a smaller fermentor volume. The use of concentrated glucose feed will also decrease the required amount of process water [25].

2.3. The fermentation–diffusion system

A coupled fermentation–diffusion system is proposed in order to prevent ethanol inhibition and increase the productivity and efficiency of the fermentation process. Several strategies have been proposed in the literature and industrial applications to prevent end-product inhibition, e.g., dialysis, vacuum, flash, extractive, membrane extractive [25] and operating the fermentor at a reduced pressure, addition of solvents and gas stripping [11]. We consider membrane separation of ethanol produced in the fermentor, it involves the use of membrane that has some selectivity for a specific product (ethanol in our case) within a reaction environment, with gas/liquid "sweep stream" on the non-reaction side to remove product away from the membrane surface. This approach has been used to remove inhibitory product (ethanol) in situ. The fermentor under investigation in this work will use an ethanol selective membrane as studied by Jeong et al. [17] where perm-selection between the substrate glucose and the product ethanol allows the efficient removal of ethanol. The ethanol permeates freely through the membrane, which is practically impermeable to the substrate [17].

2.4. Bifurcation analysis advantages

It is important to point out that carrying out bifurcation analysis, rather than simply producing dynamic simulations of the model equations for different parameter values and conditions has the following advantages:

1. For a slow process like fermentation, dynamic simulation may be inefficient, inconclusive and may not be able to locate the model characteristics that are responsible for certain rich dynamic behaviour such as bifurcation and chaos.
2. Some dynamic characteristics may be completely missed or neglected as only a limited number of dynamic simulation runs can be performed.

3. The simplified fermentation–diffusion dynamic model

We consider a homogeneous, perfectly mixed continuous culture fermentor equipped with an ethanol removal membrane for reducing product inhibition through selective ethanol removal. The configuration is schematically shown in Fig. 1.

In microbial fermentation processes, biomass acts as the catalyst for substrate conversion and is also produced by the process. An unsegregated-structured two compartment kinetic model has been developed by Jobses et al. [18–20]. This model is used in the present work for the simulation of the fermentation process. It considers biomass as being divided into two compartments containing specific groupings of macromolecules (e.g. protein, DNA and lipids), more detailed derivation is given elsewhere [2,12,13,19,20].

Considering the maintenance model [27], the substrate consumption is expressed in the following form:

$$r_S = \left(\frac{1}{Y_{SX}}\right) r_X - m_S C_X, \tag{1}$$

where the first term accounts for growth rate, and the second accounts for maintenance.

The biomass growth rate is given by its classical definition [4] as follows:

$$r_X = \mu C_X. \tag{2}$$

A proposed model for the inhibitory effect of ethanol has been given earlier [18–20]. It considers that the inhibitor does not act directly in the fermentation, but indirectly by inhibiting another reaction, which is positively linked to the product formation. This model introduces an internal key compound (e).

The proposed indirect inhibition model provides qualitatively a good description of the experimental results [19]. A quantitatively adequate model, must also account for inhibition of the total fermentation. Other models are available such as that of Ghommidh et al. [14]. Where the investigators propose that the strong fluctuations of cell viability in *Zymomonas* cultures, implies that viability is a major parameter to consider. In their approach they introduced a structured model of the cell population formed of viable, dead and non-viable cells (unable to divide but still able to produce ethanol) [14].

In the present investigation, the rate of formation of (e) is given by

$$r_e = f(C_S) f(C_P) C_e, \tag{3}$$

where the substrate dependence function $f(C_S)$ is given by the following Monod-type relation:

$$f(C_S) = \left\{\frac{C_s}{K_s + C_s}\right\}. \tag{4}$$

From experimental data [18] it is shown that the relation between alcohol concentration C_P and the alcohol dependence function $f(C_P)$ is a second-order polynomial in C_P having the following form (where k_1, k_2 and k_3 are given in Table 1):

$$f(C_P) = k_1 - k_2 C_P + k_3 C_P^2. \tag{5}$$

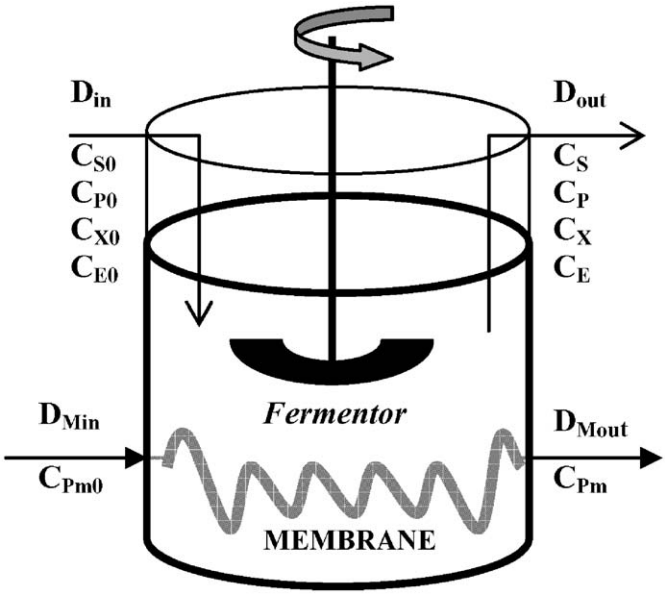

Fig. 1. The membrane fermentor.

Table 1
Base set of parameters

Parameter	Value	Remarks
C_{S_0}	140 (kg/m^3)	[2,12,13]
$D_{M_{in}}$	0.5 (h^{-1})	Section 4
A_M	0.24 (m^2)	Section 4
D_{in}	0.04 (h^{-1})	[2,12,13]
K_s	0.5 (kg/m^3)	[18–20]
k_1	16 (h^{-1})	[18–20]
k_2	0.497(m^3/kg h)	[18–20]
k_3	0.00383 (m^6/kg^2 h)	[18–20]
m_s	2.16 (kg/kg h)	[18–20]
m_p	1.1 (kg/kg h)	[18–20]
Y_{s_x}	0.0244498 (kg/kg)	[18–20]
Y_{p_x}	0.0526315 (kg/kg)	[18–20]
C_{P_0}	0(kg/m^3)	[2,12,13]
C_{e_0}	0 (kg/m^3)	[2,12,13]
C_{X_0}	0 (kg/m^3)	[2,12,13]
$C_{P_{m_0}}$	0 (kg/m^3)	Section 4
ρ	789 (kg/m^3)	[26]
V_M	0.0003 (m^3)	Section 4
V_F	0.003 (m^3)	[2,12,13]
P	0.1283 (m/h)	[17]

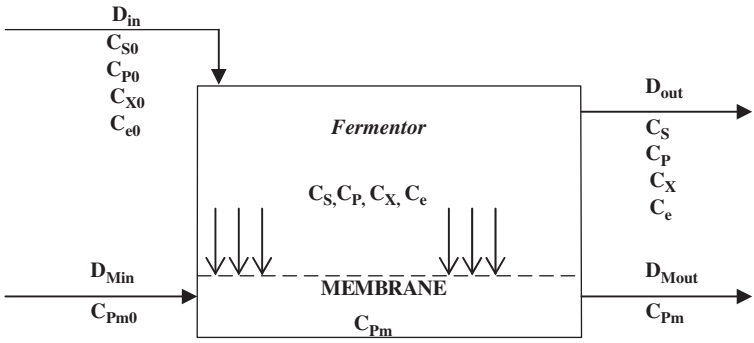

Fig. 2. The fermentation–diffusion model.

The four-dimensional model developed by Jobses (with the components: Substrate (S), product (P), microorganism biomass (X) and internal key compound (e) is extended to our membrane fermentor to include the diffusional terms for the ethanol and the differential equation for the membrane (see Fig. 2). The fifth component is the product (ethanol) in the membrane side (P_M). Our model is equivalent to the four-dimensional model when $A_M = 0$.

The unsteady state mass balance for the substrate biomass and the internal key compound are given by

$$\frac{dC_S}{dt} = \left(-\frac{1}{Y_{SX}}\right)\left\{\frac{(C_s C_e)}{(K_s + C_s)}\right\} - m_S C_X + D_{in} C_{S_0} - D_{out} C_S, \tag{6}$$

$$\frac{dC_X}{dt} = \left\{\frac{(C_s C_e)}{(K_s + C_s)}\right\} + D_{in} C_{X_0} - D_{out} C_X, \tag{7}$$

$$\frac{dC_e}{dt} = \{k_1 - k_2 C_P + k_3 C_P^2\}\left\{\frac{(C_s C_e)}{(K_s + C_s)}\right\} + D_{in} C_{e_0} - D_{out} C_e. \tag{8}$$

Note that the inlet dilution rate and the output dilution rate for the fermentor are not equal because of the ethanol removal through the membrane, which reduces the total flow rate in the fermentor.

The planned experimental setup will have the provision of introducing a membrane module inside the fermentor. The dilution flow rate is chosen at high values in order to enhance the ethanol removal and make the concentration gradient negligible along the length of the membrane tube. This assumption makes the diffusional driving force constant along the membrane length and therefore simplifies the model considerably by keeping it as a lumped model without introducing distributed components.

The unsteady state mass balances for the product (ethanol) on the fermentor and the membrane are given by

$$\frac{dC_P}{dt} = \left(\frac{1}{Y_{PX}}\right)\left\{\frac{(C_s C_e)}{(K_s + C_s)}\right\} + m_P C_X + D_{in} C_{P_0} - D_{out} C_P - \left(\frac{A_M P}{V_F}\right)(C_P - C_{P_m}), \tag{9}$$

$$\frac{dC_{P_m}}{dt} = \left(\frac{A_M P}{V_M}\right)(C_P - C_{P_m}) + D_{M_{in}} C_{P_{m_0}} - D_{M_{out}} C_{P_m}. \tag{10}$$

where A_M is the permeation area and P the membrane permeability for the ethanol.

Using an overall mass balance for the fermentor we obtain the necessary simple relation for the outgoing fermentor dilution rate

$$D_{out} = D_{in} - \frac{A_M P(C_P - C_{P_m})}{V_F \rho}, \tag{11}$$

where ρ is the ethanol density, V_F is the operation fermentor volume, and D_{in} is the inlet fermentor dilution rate.

In the same fashion, using an overall mass balance for the membrane, the outgoing dilution rate for the membrane is given by

$$D_{M_{out}} = D_{M_{in}} + \frac{A_M P(C_P - C_{P_m})}{V_M \rho}, \tag{12}$$

where V_M is the membrane volume and $D_{M_{in}}$ is the inlet membrane dilution rate.

The coupled diffusion/fermentation model is thus represented by the set of five differential equations, (6)–(10), coupled with the two algebraic equations (11) and (12), and has 20 parameters (Table 1 gives the base set of parameters).

4. Identification of parameter values

The planned experimental setup will have the provision of introducing a membrane module inside the fermentor, with a volume of about 10% the fermentor active volume (since $V_F = 0.003\,m^3$, then $V_M = 0.0003\,m^3$). $D_{M_{in}}$ is chosen high in order to enhance the ethanol removal, and keep constant the diffusional driving force along the membrane for model simplification purposes as explained in Section 3 ($D_{M_{in}} = 0.5\,h^{-1}$). The area of membrane is set at a high value in order to keep a high rate (using a relatively small diameter for the membrane to give a high surface per unit volume) of ethanol removal ($A_M = 0.24\,m^2$).

5. Computational resources and numerical tools for nonlinear analysis

5.1. Simulations

Mathematica 4.1. [29] was used for obtaining the system steady states for a particular set of parameters. Those steady states were used as the starting points for AUTO97. The built in commands in the computational package Mathematica are not efficient for finding all the roots of this five-dimensional set of nonlinear algebraic equations, requiring very long computational times. In order to overcome this problem, the developed program is arranged to "not to ask" this software to find all the solutions (as the built in routine does), but to find them using an intelligently chosen initial guess.

The program uses a loop that generates a random initial condition on each state variable for a large range of possible solutions. All the steady states for a given set of parameters are found in a "probabilistic way" more efficiently that the "deterministic" built in method.

Polymath 5.0 [8] is used for simulation purposes; obtaining the time traces and phase planes in regions with periodic attractors.

5.2. Bifurcation analysis

Both static and dynamic bifurcations have been investigated using three parameters, namely the inlet glucose concentration, the inlet fermentor dilution rate and the inlet membrane dilution rate (C_{S_0}, D_{in} and $D_{M_{in}}$). For this purpose we used the Linux program XPPAUT 5.0 [10] as a support for the bifurcation program AUTO97 [7]. This package is able to perform both steady state and dynamic bifurcation analysis, including the determination of entire periodic branches, starting at Hopf bifurcation (HB) points and terminating at homoclinical (infinite period) termination (HT).

6. Bifurcation analysis

This experimentally verified model predicts static as well as periodic bifurcation behaviour. Periodic attractors exist over a relatively wide range of parameters. From a phenomenological perspective, oscillatory behaviour (periodic attractors as well as multiplicity of steady states) arise from the interaction between cell growth, glucose consumption and the ethanol production. Bifurcation characterizations are investigated using the bifurcation analysis package AUTO97. The resources discussed earlier are utilized to investigate the rich dynamic behaviour of the system.

6.1. Definition of some key operation variables

In order to account for the complete behaviour of the system, some auxiliary variables are defined as follows:

The glucose conversion is defined as the ratio between the actual rate of glucose consumption by the bacteria, and the rate of glucose supply. For computing this overall variable

we use

$$X_S = \left\{ \frac{C_{S_0} D_{in} V_F - C_S D_{out} V_F}{C_{S_0} D_{in} V_F} \right\}. \tag{13}$$

The ethanol production rate is defined as the combined productivity coming from both, the fermentor and the membrane output. For computing this overall variable we use

$$P_P = C_P D_{out} V_F + C_{P_m} D_{M_{out}} V_M. \tag{14}$$

The product yield is defined as the ratio between the production rate and glucose supply rate into the fermentor. For computing this overall variable we use

$$Y_P = \left\{ \frac{P_P}{C_{S_0} D_{in} V_F} \right\}. \tag{15}$$

The rate of ethanol removal from the fermentor to the membrane side is defined as the productivity from the membrane side. For computing this overall variable we use

$$R_{ER} = C_{P_m} D_{M_{out}} V_M. \tag{16}$$

Average values for periodic attractors are computed for the substrate and ethanol concentrations in the fermentor side, the ethanol concentration in the membrane side, the glucose conversion, the ethanol yield and production rate, and the rate of ethanol removal. For computing these averaged variables after a Hopf bifurcation, a simple mean is used as follows:

$$\overline{C_i} = \int_a^{a+\tau} \frac{C_i(t)}{\tau}\,dt, \quad \overline{X_S} = \int_a^{a+\tau} \frac{X_S(t)}{\tau}\,dt, \quad \overline{Y_P} = \int_a^{a+\tau} \frac{Y_P(t)}{\tau}\,dt,$$
$$\overline{P_P} = \int_a^{a+\tau} \frac{P_P(t)}{\tau}\,dt, \quad \overline{R_{ER}} = \int_a^{a+\tau} \frac{R_{ER}(t)}{\tau}\,dt, \tag{17}$$

where "a" is the chosen time for starting the average computation after the disappearance of all initial transients, and τ is the oscillation period.

7. Results and discussion

The results are classified into two sections (with/without ethanol removal membrane). What follows is an outline of the analyzed cases:

A. *Fermentation without ethanol removal* ($A_M = 0\,m^2$), static and dynamic bifurcations):

Case (A.1): Dilution rate D_{in} as the bifurcation parameter.
Case (A.2): Inlet substrate concentration C_{S_0} as bifurcation parameter.

B. *Fermentation with continuous ethanol removal*:

Case (B.1): Inlet substrate concentration C_{S_0} as bifurcation parameter.

(At high inlet membrane dilution rate, all bifurcation phenomena disappears giving rise to high sugar conversion and high ethanol yield in a unique stable steady state).

Case (B.2): Inlet membrane dilution rate $D_{M_{in}}$ as the bifurcation parameter. (Dynamic bifurcation only).

Case (B.3): Inlet membrane dilution rate $D_{M_{in}}$ as the bifurcation parameter. (Static and dynamic bifurcations).

For the cases of "fermentation without ethanol removal", the bifurcation analysis is carried out for two different bifurcation parameters: D_{in} (fermentor dilution rate) and C_{S_0} (inlet feed substrate concentration). For the non-membrane configuration (cases (A.1) and (A.2)), only a sample of the complete work from Garhyan et al. [13] will be discussed.

For the cases of "fermentation with continuous ethanol removal", the bifurcation analysis is carried out for two different bifurcation parameters: C_{S_0} (inlet feed substrate concentration) and $D_{M_{in}}$ (membrane dilution rate).

The reason for choosing these three bifurcation parameters (D_{in}, C_{S_0} and $D_{M_{in}}$) is that they are the easiest ones to manipulate experimentally during the operation of a laboratory or full-scale fermentor. For each case, all of the parameters (other than the bifurcation parameter) were kept constants at the values in Table 1. The default values in Table 1 are used unless the contrary is mentioned.

Figs. 3, 5, 7, 8 and 9 are bifurcation diagrams (in Fig. 7 all bifurcation phenomena disappear) for some chosen state variables such as: The fermentor glucose concentration (C_S), ethanol concentration in the fermentor side (C_P), ethanol concentration in the membrane side (C_{P_m}), fermentor internal key compound concentration (C_e), fermentor biomass concentration (C_X), the glucose conversion (X_S), ethanol yield (Y_P), production rate (P_P) and the rate of ethanol removal (R_{ER}). The average values for the periodic branch ($\overline{C_S}$, $\overline{C_P}$, $\overline{C_{P_{in}}}$, $\overline{X_S}$, $\overline{Y_P}$, $\overline{P_P}$, and $\overline{R_{ER}}$) are shown as diamond shaped points. Figs. 4, 6 and 10 show the period of oscillations as the periodic branch approaches homoclinical termination point; the period tends to infinity indicating the homoclinical termination of the periodic attractor [21].

The effectiveness of the ethanol removal membrane is clearly evaluated in cases (A.2) and (B.1). A case without membrane for comparison purposes (case A.2), and a high membrane dilution rate case $D_{M_{in}} = 0.5$ (case B.1) are evaluated. A summary of the results on each case is shown in Table 2. The case (B.1), is analyzed in detail. It shows the stabilizing effect of the membrane, as we increase its inlet dilution rate all bifurcation phenomena disappears, removing multiplicity of steady states, eliminating periodic attractors and changing them into stable fixed point attractors. The results are compared for $140\,kg/m^3$ of inlet glucose concentration. This value was chosen because this was one of the concentrations for which kinetic data was developed by Jobses et al. [18–20].

Regarding the evaluation of the effect of the ethanol removal membrane (and its inlet membrane dilution rate) two more cases are investigated. In both cases the inlet membrane dilution rate is the bifurcation parameter. In the first case the inlet sugar concentration is $C_{S_0} = 140\,kg/m^3$ (case B.2), and for the second case the inlet sugar concentration is $C_{S_0} = 160\,kg/m^3$ (case B.3). A summary of the qualitative results on each case is shown in Table 3. Cases (B.2) and (B.3) are investigated to show the effect of the membrane as

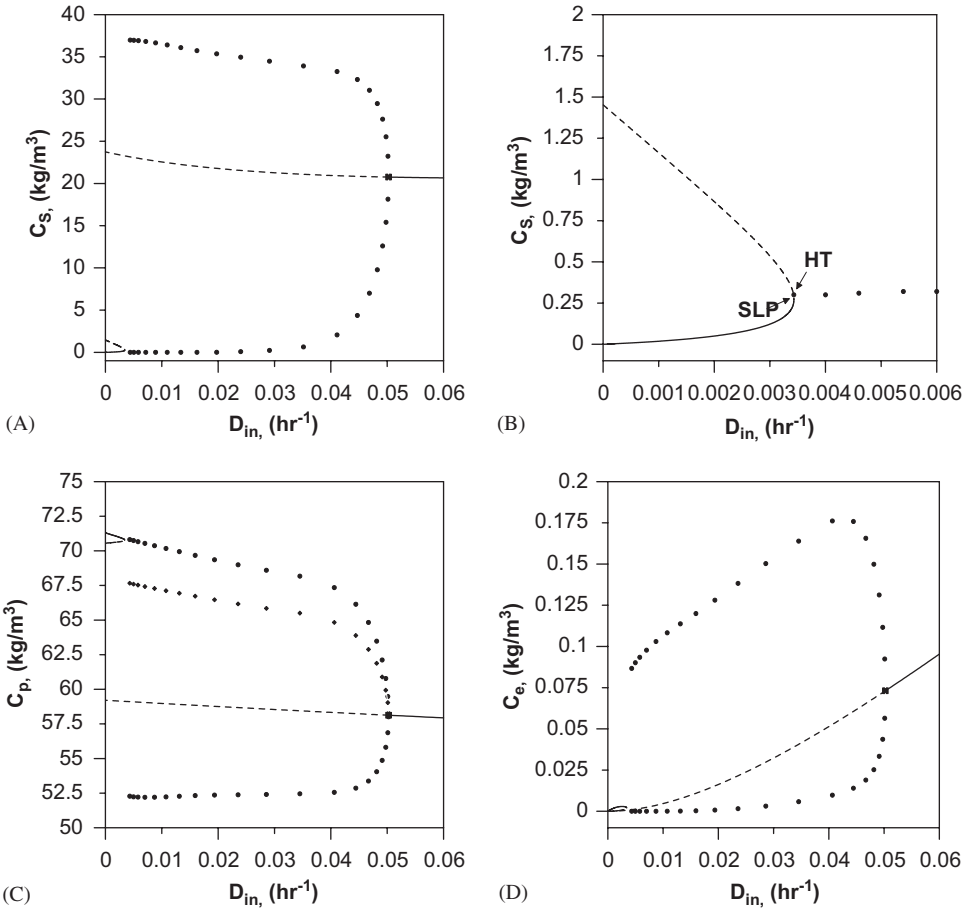

Fig. 3. Bifurcation diagrams including oscillations averages (inlet fermentor dilution rate as the bifurcation parameter, $A_M = 0\,m^2$, $C_{S_0} = 140\,kg/m^3$): (a) glucose concentration; (b) zoom of (a); (c) fermentor ethanol concentration; (d) internal key compound concentration; (e) biomass concentration; (f) glucose conversion; (g) ethanol yield. Steady state branch (stable: _____, unstable: – – – – –, periodic branch (stable: ●●●●●, average of oscillations: ♦♦♦♦♦). HB: Hopf bifurcation, HT: Homoclinical termination, SLP: Static limit point.

a system stabilizer using the membrane dilution rate as the bifurcation parameter. In both cases the effect of the increase of the membrane dilution rate is discussed as well as its advantage as a system stabilizer and ethanol productivity enhancer. Case (B.2) is chosen as a case with dynamic bifurcation, but without static bifurcation. Case (B.3) is chosen as a case having both static and dynamic bifurcations.

7.1. Fermentation without ethanol removal (area of permeation $A_M = 0$)

For this case, a four-dimensional system is considered [2,13]. It is equivalent to our five-dimensional model when the permeation through the membrane is set equal to zero.

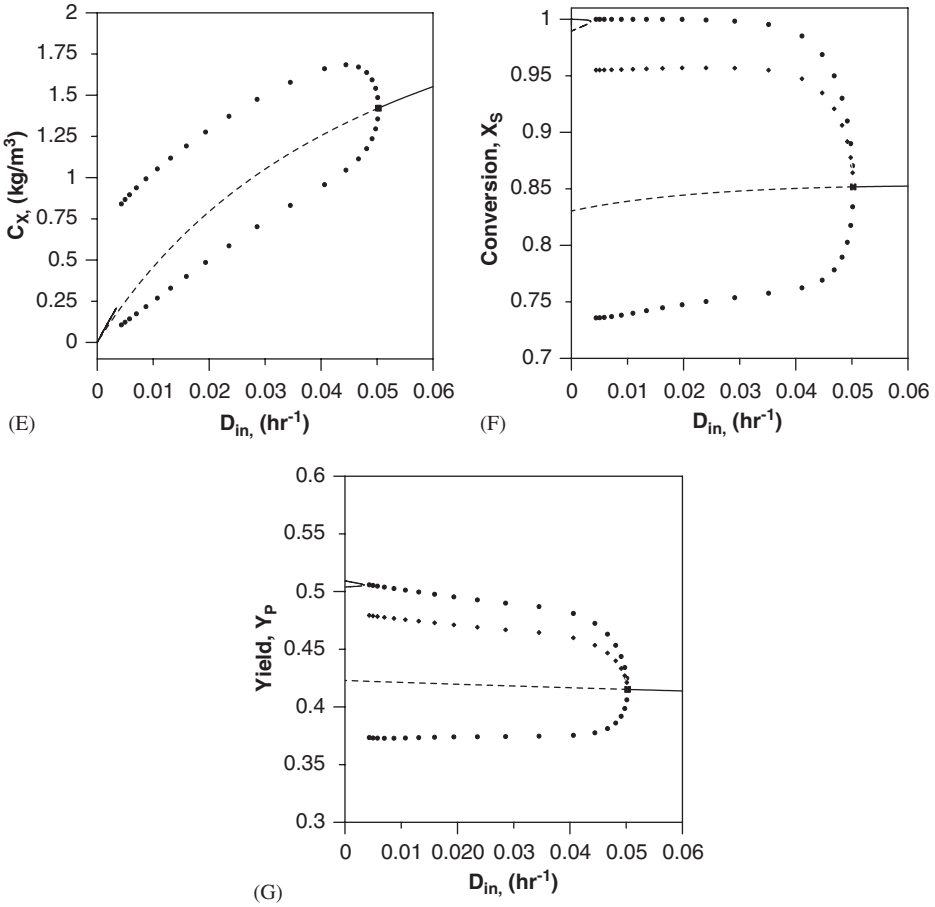

Fig. 3. (*Continued*).

In this case, inlet and outlet fermentor dilution rates are equal (Eq. (11)) and the membrane equations (Eqs. (10) and (12)) disappear. Details for the static and dynamic bifurcation are shown as a sample for our comparison regarding the improvement of the membrane configuration.

7.1.1. Case (A.1): Dilution rate D_{in} as the bifurcation parameter ($A_{\text{M}} = 0\,\text{m}^2$, $C_{\text{S}_0} = 140\,\text{kg/m}^3$)

Jobses and coworkers [18–20] used in their experiments this value of C_{S_0} together with a dilution rate $D_{\text{in}} = 0.022\,\text{h}^{-1}$. Details for static and dynamic bifurcation behaviour for this case are given in Figs. 3(a)–(g), with the dilution rate D_{in} as the bifurcation parameter, with values varying around the experimental value of $D_{\text{in}} = 0.022\,\text{h}^{-1}$.

Fig. 3(a) shows the bifurcation diagram for substrate concentration (C_{S}). It is clear that the static bifurcation diagram is an incomplete *S*-shape hysteresis type with a static limit

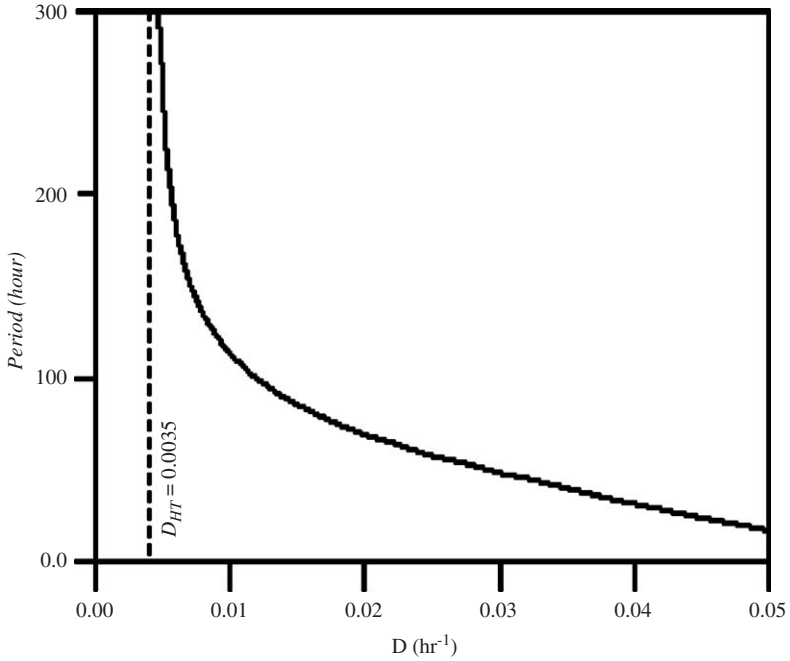

Fig. 4. Period of oscillations for the periodic branch ($A_M = 0\,m^2$, $C_{S_0} = 140\,kg/m^3$). HB. Hopf bifurcation, HT: Homoclinical termination.

Table 2
Inlet substrate concentration as bifurcation parameter

Case with $C_{S_0} = 140$ (kg/m^3)	Description	Dynamics	$\overline{X_S}$	$\overline{Y_P}$	$\overline{P_P}$ (g/h)	Improvement compared with case A.2
A.2	Without membrane	Multiplicity of steady states at high Inlet substrate concentration, Hopf bifurcation and homoclinical termination of the periodic branch	Periodic branch: 0.89	Periodic branch: 0.431	Periodic branch: 7.2948	—
B.1	Membrane: $D_{M_{in}} = 0.5\,h^{-1}$	All bifurcation phenomena disappear.	Point attractor: 0.99994	Point attractor: 0.4938	Point attractor: 8.3614	For $\overline{F_S}$: 12.35%, For $\overline{Y_P}$: 14.57%, and for $\overline{P_P}$: 14.62%

Improvements of the membrane case.

Table 3
Inlet membrane dilution rate as a bifurcation parameter (membrane fermentor)

Case	Description	Dynamics
B.2	$C_{S_0} = 140\,\mathrm{kg/m^3}$	Hopf bifurcation, oscillations eliminated with the increase of $D_{M_{in}}$
B.3	$C_{S_0} = 160\,\mathrm{kg/m^3}$	Multiplicity of steady states at low inlet membrane dilution rate, Hopf bifurcation and homoclinical termination of the periodic branch, oscillations eliminated with the increase of $D_{M_{in}}$

point (*SLP*) at very low value of $D_{in} = 0.0035\,h^{-1}$. The dynamic bifurcation shows a Hopf bifurcation point (*HB*) at $D_{in}=0.05\,h^{-1}$ with a periodic branch emanating from it. The region in the neighborhood of the *SLP* is enlarged in Fig. 3(b). It is clear that the periodic branch emanating from *HB* terminates homoclinically (with infinite period) when it touches the saddle point very close to the *SLP* at $D_{in} = 0.0035\,h^{-1}$. Figs. 3(d) and (e) are the bifurcation diagrams for the internal key component e, concentration (C_e) and biomass concentration (C_X), respectively. Fig. 3(c) is the bifurcation diagram for the ethanol concentration (C_P). It is clear from Fig. 3(c) that the average ethanol concentrations for the periodic attractors are higher than the corresponding unstable steady states. Figs. 3(f)–(g) show the bifurcation diagrams for substrate conversion (X_s), and ethanol yield (Y_P). The average conversion ($\bar{X}_S$) and yield ($\bar{Y}_P$) for periodic branch are shown as diamond-shaped points in Figs. 3(f)–(g). Fig. 4 shows the periods of oscillation as the periodic branch approaches the homoclinical bifurcation point. The period tends to infinity indicating homoclinical termination of the periodic attractor[25] at $D_{in} = 0.0035\,h^{-1}$.

The bifurcation diagram in this case can be divided into three regions:

7.1.1.1. The first region. It includes the range of $D_{in} > D_{in_{HB}}$, where $D_{in_{HB}} = 0.05\,h^{-1}$. In this region there is a unique stable point attractor. At $D_{HB}=0.05\,h^{-1}$ sugar conversion is $X_S=0.85$ and sugar concentration is $C_S=20.997\,\mathrm{kg/m^3}$. C_S decreases (while the conversion increases) slightly with D_{in} increase as shown in Figs. 3(a) and (f). The yield of ethanol is $Y_P=0.415$ and the ethanol concentration is $C_P=58.035\,\mathrm{kg/m^3}$ at $D_{in_{HB}}$ and they decrease slowly with the increase in D_{in} as shown in Figs. 3(c) and (g).

7.1.1.2. The second region. This region includes the range of $D_{in_{HB}} > D_{in} > D_{in_{HT}}$, (i.e. $0.05 > D_{in} > 0.0035$). In this region there is a unique periodic attractor (surrounding the unique unstable steady state) which starts at the *HB* point and terminates homoclinically at a point very close to *SLP* at $D_{in} = 0.0035\,h^{-1}$ as shown in Figs. 3(a)–(g).

For the unstable steady state branch, the sugar concentration (C_S) in this region increases with the decrease of D_{in} from 20.997 to $23.992\,\mathrm{kg/m^3}$ as shown in Fig. 3(a) Similarly the yield of ethanol (Y_P) increases from 0.415 to 0.425 as shown in Fig. 3(g). Ethanol concentration (C_P) increases slightly from 58.035 to $59.235\,\mathrm{kg/m^3}$ as shown in Fig. 3(c). For the periodic branch, the amplitudes of the oscillations are quite large for all state variables. The average sugar conversion varies between 0.85 and 0.878 (shown as the diamond-

shaped points in Fig. 3(f)). The average ethanol concentration $\bar{C}_P$ varies between 59.315 and 61.532 kg/m^3 (Fig. 3(c)), while the average ethanol yield ($\bar{Y}_P$) values are varying in this region between 0.447 and 0.42 (Fig. 3(g)).

It is clear that in this region, the average of the oscillations for the periodic attractor gives (as shown in Figs. 3(c) and (f)–(g)) higher $\bar{C}_P$, $\bar{X}_S$ and $\bar{Y}_P$ than that of the corresponding steady states which means that the operation of the fermentor under periodic conditions in this region is not only more productive but will also give higher ethanol concentrations by achieving better sugar conversion. Comparison between the values of the static branch and the average of the periodic branch at $D_{in} = 0.045\,h^{-1}$ shows that the percentage improvements are as follows: for $\bar{C}_P$ it is 9.34%, for $\bar{X}_S$ it is 9.66% and for $\bar{Y}_P$ it is 8.67%.

7.1.1.3. The third region. For $D_{in} < 0.0035\,h^{-1}$, there are three steady states, two of them are unstable and only the steady state with the highest conversion is stable. The highest conversion (almost complete conversion) occurs in this region for the high conversion stable steady state, and also it gives the highest ethanol yield, which is equal to 0.51 (Figs. 3(f) and (g)).

The upper steady state (in the multiplicity region) gives the highest ethanol concentration and yield as compared with all other steady states (including the average of periodic attractors (Figs. 3(c) and (g)). However, it occurs at a very narrow region at very low D_{in} (i.e. very low q_{in}/V_F), thus its ethanol production rate per unit volume of fermentor is drastically low. Therefore, the best production policy for ethanol concentration, yield and productivity is in the periodic attractors region.

In general, there is a trade-off between concentration and productivity, which requires economic optimization study to determine the optimum D_{in}. However, such an optimization study will have to take into consideration the fact that some periodic attractors have higher ethanol yield and production rate than the corresponding steady states.

7.1.2. Case (A.2): Inlet substrate concentration C_{S_0} as bifurcation parameter ($A_M = 0\,m^2$, $D_{in} = 0.04\,h^{-1}$)

As we increase the inlet glucose concentration, process behaviour can be divided into the following regions:

7.1.2.1. The first region: At low inlet glucose concentration in the range: [$C_{S_0} < 127.92$ kg/m^3]. In this region we have a unique stable steady state (unique point attractor). Here the microorganisms consume almost all of the provided substrate; giving rise to nearly 100% glucose conversion. Also it is clear that the ethanol concentration increases inside the fermentor (Fig. 5(a)). The maximum fermentor ethanol concentration in this region is 58.29 kg/m^3; just before a Hopf bifurcation occurs (region two).

At low glucose concentration (lower than 116 kg/m^3), the substrate conversion is near 0.99, but as we increase the glucose inlet concentration up to 127.92 kg/m^3, the conversion decreases 6.68% to a value of X_S=0.9281. In this region (116 kg/m^3 < C_{S_0} < 127.92 kg/m^3) it is clear that any increase in the feed glucose concentration lowers the glucose conversion, keeping almost constant the product concentration as well as the productivity.

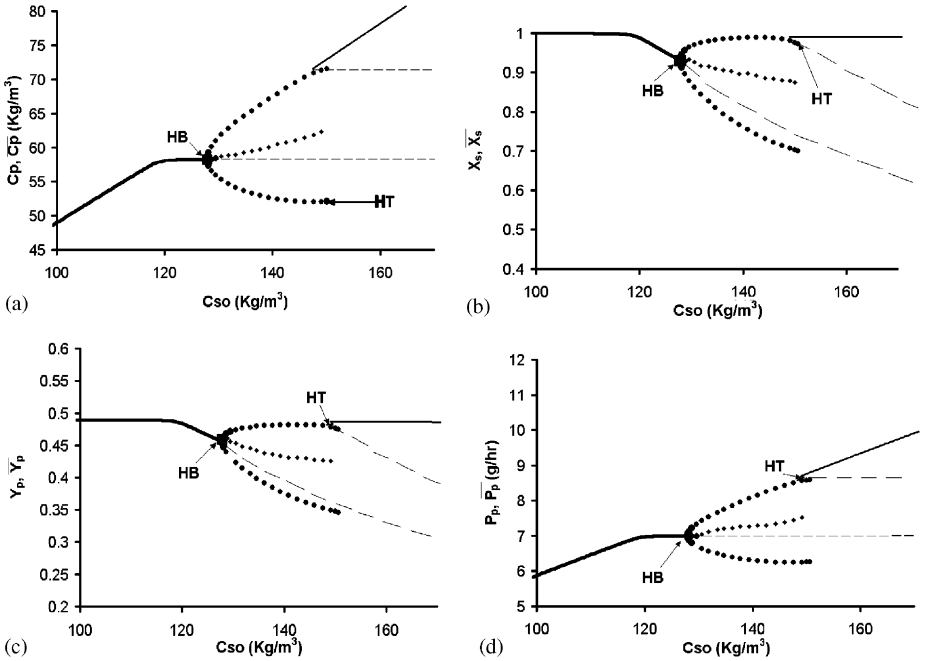

Fig. 5. Bifurcation diagrams including oscillations averages (inlet glucose concentration as the bifurcation parameter, $A_M = 0\,m^2$, $D_{in} = 0.04\,h^{-1}$): (a) fermentor ethanol concentration; (b) glucose conversion; (c) ethanol yield; (d) ethanol production rate. Steady state branch (stable: _____, unstable: – – – – –), periodic branch (stable: ●●●●●, average of oscillations: ♦♦♦♦♦). HB: Hopf bifurcation, HT: Homoclinical termination.

7.1.2.2. The second region: Inlet glucose concentration in the range: $[127.92\,kg/m^3 < C_{S_0} < 150.032\,kg/m^3]$. This region is covered by a periodic branch. A Hopf bifurcation appears giving rise to oscillations with increasing amplitude. The averages for those oscillations were computed showing a decrease on the glucose conversion (Fig. 5(b)) as well as the ethanol yield (Fig. 5(c)) compared with the first region. As an example; the glucose conversion decreases from 0.928 (just before the Hopf bifurcation) to 0.875 (as the oscillation average at the end of the periodic branch), this corresponds to a 6.05% decrease. The product yield decreases from 0.4571 to 0.4261, corresponding to a 7.27% decrease. It is also very important to notice that the oscillation averages give higher product concentration, substrate conversion, ethanol yield, and ethanol productivity than what can be achieved by the corresponding unstable steady states. The oscillatory behaviour in this region improves the fermentation process because the oscillation averages give higher productivity than their corresponding steady states.

This periodic branch touches a steady state branch at $C_{S_0} = 150.032\,kg/m^3$ (Figs. 5(a)–(d)). Here the periodic branch that emanates from $C_{S_0} = 127.92\,kg/m^3$ disappears in a phenomenon called homoclinical termination (with infinite period). Fig. 6 shows the period of oscillations as the periodic branch approaches homoclinical termination point; the period tends to infinity indicating the homoclinical termination of the periodic attractor.

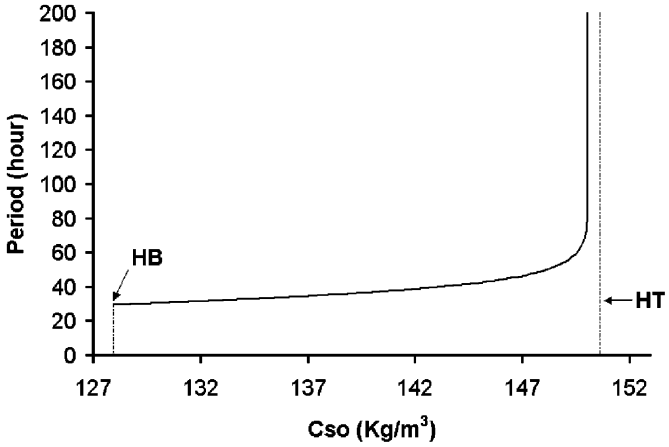

Fig. 6. Period of oscillations for the periodic branch ($A_M = 0\,m^2$, $D_{in} = 0.04\,h^{-1}$). HB: Hopf bifurcation, HT: Homoclinical termination.

7.1.2.3. The third region: Inlet glucose concentration in the range: $[C_{S_0} > 150.032\,kg/m^3]$. In this region there are three steady states, only one of them is stable having the same behaviour as described in the first region. It is a high conversion steady state having an almost constant conversion of 0.99. It also gives the highest ethanol yield, which is 0.486. (Figs. 5(b), (c)). Here, we can see that the increase of the inlet glucose concentration increases the productivity (Fig. 5(d))) maintaining the efficiency almost constant at a very high value.

7.2. Fermentation with continuous ethanol removal

In the previous section, bifurcation analysis of the four-dimensional system (without continuous ethanol removal) has been carried out based on two different bifurcation parameters, namely, dilution rate (D_{in}, h^{-1}) and feed sugar concentration $C_{S_0}, kg/m^3$). To improve the productivity and yield, continuous removal of ethanol will now be incorporated in our analysis. Bifurcation study is carried out for such a system having the inlet feed substrate concentration (C_{S_0}, kg/m^3) and the membrane dilution rate ($D_{M_{in}}$, h^{-1}) as the bifurcation parameters.

7.2.1. Case (B.1): Inlet substrate concentration C_{S_0} as bifurcation parameter ($A_M = 0.24\,m^2$, $D_{in} = 0.04\,h^{-1}$, $D_{M_{in}} = 0.5\,h^{-1}$)

For this case there is only one region of unique steady state for all the parameter range. There is neither static nor dynamic bifurcation. It is clear that the membrane has a strong stabilizing effect. There is no bifurcation and the fermentor operates in a unique steady state for any value of the feed glucose concentration. The multiplicity region and all the oscillations also disappear.

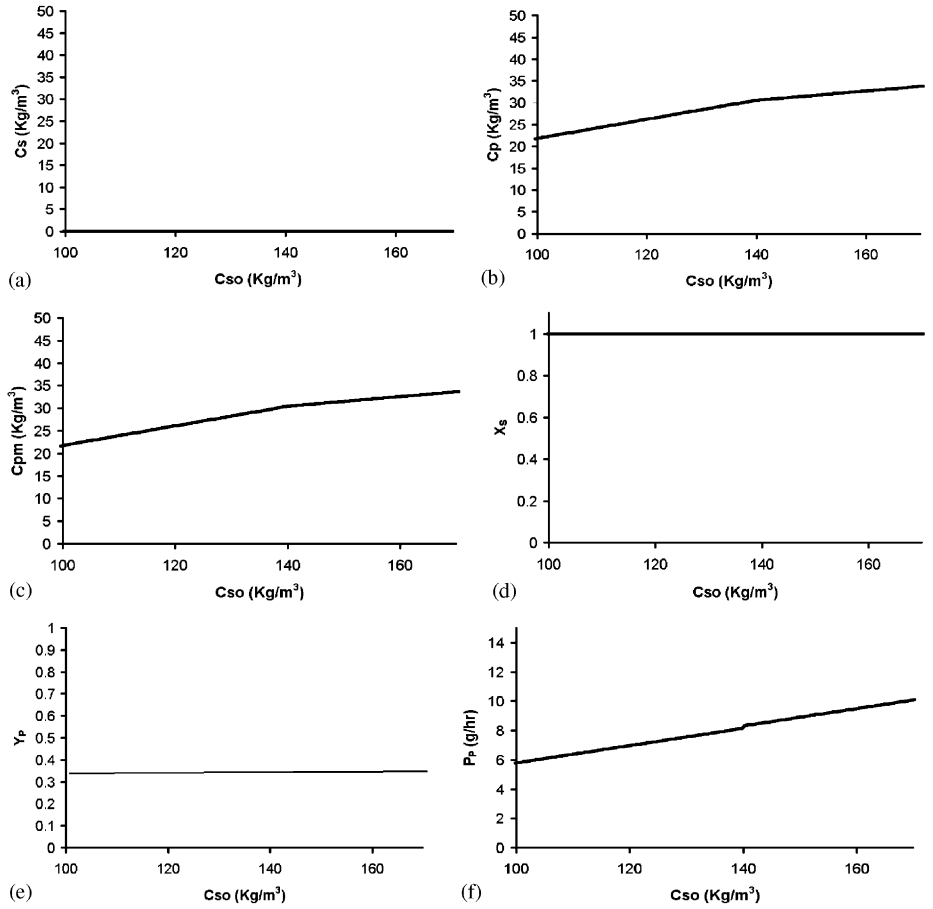

Fig. 7. Bifurcation diagrams where all bifurcation phenomena disappears (inlet glucose concentration as the bifurcation parameter, $A_M = 0.24\,m^2$, $D_{in} = 0.04\,h^{-1}$, $D_{M_{in}} = 0.5\,h^{-1}$): (a) fermentor glucose concentration; (b) fermentor ethanol concentration; (c) membrane ethanol concentration; (d) glucose conversion; (e) ethanol yield; (f) ethanol production rate. Stable steady state branch (_____).

At inlet glucose concentrations lower than $140\,kg/m^3$ the fermentor sugar concentration remains practically constant at a value of zero corresponding to 100% conversion ($X_S = 1$). The fermentor outlet ethanol concentration (Fig. 7(b)), increases in direct proportion to the increase of C_{S_0}. The difference between the ethanol concentration inside the membrane and on the fermentor is almost negligible (Fig. 7(c)).

For $C_{S_0} > 140\,kg/m^3$, the sugar conversion (Fig. 7(d)) remains almost constant at 0.9999. The yield factor (Fig. 7(e)) remains almost constant at 0.495. And the production rate (Fig. 7(f)) increases in linearly with the increase of the inlet glucose concentration, giving values up to 10.077 g/h.

The overall improvement of case (B.1) over (A.2) is summarized in Table 2.

7.2.2. Case (B.2): Inlet membrane dilution rate $D_{M_{in}}$ as the bifurcation parameter ($A_M = 0.24\,m^2$, $D_{in} = 0.04\,h^{-1}$, $C_{S_0} = 140\,kg/m^3$)

7.2.2.1. The first region: Inlet membrane dilution rate in the range: $[D_{M_{in}} < 0.0399929\,h^{-1}]$. This region is dominated by a periodic branch. As we increase the inlet membrane dilution rate up to $D_{M_{in}} = 0.0399929\,h^{-1}$ a Hopf bifurcation appears (Fig. 8). The averages for those oscillations were computed showing a continuous increase in the glucose conversion (Fig. 8(d)) as well as the yield, production rate, and rate of ethanol removal (Figs. 8(e)–(g)). It is important to notice that the average conversion and ethanol productivity and product yield for the periodic attractors are higher than the corresponding (unstable) steady states.

When $D_{M_{in}}$ goes to zero; the system has strong sustained oscillations. At this point, there is no flow into the membrane, the rate of ethanol removal goes to zero (Fig. 8(g)), and the system behaviour is equivalent to a non-membrane fermentor.

7.2.2.2. The second region: Inlet membrane dilution rate in the range: $[D_{M_{in}} > 0.0399929\,h^{-1}]$. In this region there is a unique stable steady state. Here the microorganisms consume almost all of the provided substrate; giving rise to very high substrate conversions, between 90% and 100%, at high values of the membrane dilution rate. This phenomenon can be seen on Fig. 8(a) where the substrate concentration inside the fermentor is between 10 and $0.0\,kg/m^3$ (at $D_{M_{in}} > 0.07$). Also the overall effect is shown in Figs. 8(d)–(g) where the positive effect is clear of flow increase inside the membrane ($D_{M_{in}}$) for the fermentation process. Not only that it stabilizes the system (destroy oscillations) but it also increases the substrate conversion (up to 0.999), ethanol yield (up to 0.485) and product rate (up to 7.87 g/h) (Figs. 8(e)–(f)).

For the evaluation of the membrane, we compare the process when the membrane dilution rate is zero with a high dilution rate; at say $D_{M_{in}} = 0.07$ (Table 4). The percentage of improvement in the efficiency of the fermentation process is around 11.66%.

7.2.3. Case (B.3): Inlet membrane dilution rate $D_{M_{in}}$ as the bifurcation parameter ($A_M = 0.24\,m^2$, $D_{in} = 0.04\,h^{-1}$, $C_{S_0} = 160\,kg/m^3$)

7.2.3.1. The first region: Inlet membrane dilution rate in the range: $[D_{M_{in}} < 0.0361\,h^{-1}]$ This region has three steady states with a unique high conversion stable steady state. It consists of a high conversion steady state (Fig. 9(d)) at an almost constant conversion of 0.999. It also gives a high ethanol yield, which is 0.489. (Fig. 9(e)). Here it is clear that the increase of the inlet glucose concentration, increases the productivity maintaining the efficiency at a very high value.

7.2.3.2. The second region: Inlet membrane dilution rate in the range: $[0.0361\,h^{-1} < D_{M_{in}} < 0.09827\,h^{-1}]$ This region is dominated by a periodic branch. As we increase the inlet membrane dilution rate up to $D_{M_{in}} = 0.09827\,h^{-1}$ a Hopf bifurcation appears (Fig. 9). The averages for those oscillations were computed showing a low decrease on the glucose conversion (Fig. 9(d)) as well as the ethanol yield, production rate, and rate of ethanol removal (Figs.

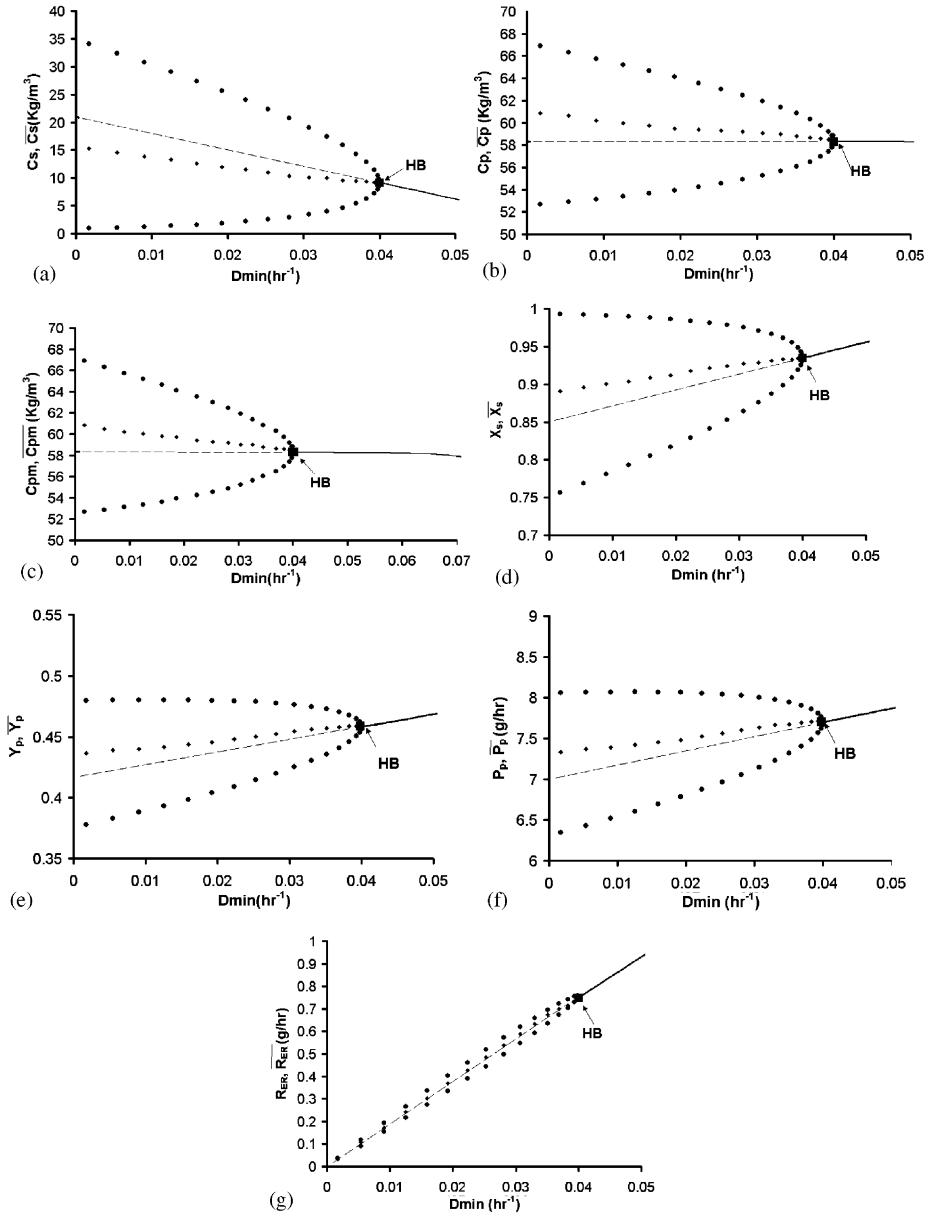

Fig. 8. Bifurcation diagrams including oscillations averages (inlet membrane dilution rate as the bifurcation parameter, $A_M = 0.24\,m^2$, $D_{in} = 0.04\,h^{-1}$, $C_{S_0} = 140\,kg/m^3$): (a) Fermentor glucose concentration, (b) fermentor ethanol concentration; (c) membrane ethanol concentration; (d) glucose conversion; (e) ethanol yield; (f) ethanol production rate; (g) rate of ethanol removal. Steady state branch (stable: _____, unstable: – – – – –), periodic branch (stable: ● ● ● ● ●, average of oscillations: ♦♦♦♦♦). HB: Hopf bifurcation.

Table 4
Membrane improvements using high inlet membrane dilution rates

Variable (Case B.2)	Average value ($D_{M_{in}} = 0$)	Value ($D_{M_{in}} = 0.07$)	Improvement
P_P	7.3344	8.189591	11.659%
Y_P	0.4365	0.487476	11.678%
X_S	0.89	0.993888	11.672%

9(e)–(g)). It is also very important to notice that the oscillation averages give higher product concentration, substrate conversion, ethanol yield, and ethanol productivity than what can be achieved at their corresponding unstable steady states. Although globally the efficiency in this region is lower than in region 1 (see the unstable steady states), the oscillatory behaviour in this region improves the fermentation process because the oscillation averages give higher productivity than their corresponding steady states.

This oscillating branch touches a steady state branch at $D_{M_{in}} = 0.0361\,h^{-1}$. Here the periodic branch that emanates from $D_{M_{in}} = 0.09827\,h^{-1}$ disappears homoclinically (with infinite period). Fig. 10 shows the period of oscillations as the periodic branch approaches the homoclinical termination point (the period tends to infinity indicating the homoclinical termination of the periodic attractor).

7.2.3.3. The third region: Inlet membrane dilution rate in the range: $[D_{M_{in}} > 0.09827\,h^{-1}]$. In this region there is a unique stable steady state. Here the microorganisms consume almost all of the provided substrate; giving rise to very high substrate conversions, near 100% at high values of the membrane dilution rate ($D_{M_{in}} > 0.147$). This phenomenon is clearly shown in Fig. 9(a) where the substrate concentration inside the fermentor is near zero ($D_{M_{in}} > 0.147$). Also the overall effect can be seen in Figs. 9(d)–(g), where we can see the positive effect of the increase of the flow inside the membrane ($D_{M_{in}}$) for the fermentation process. It stabilizes the system (avoid oscillations as shown in region two) and increases the substrate conversion (up to 0.999), ethanol yield (up to 0.4898) and production rate (up to 9.411 kg/h) (Figs. 9(e)–(f)).

As we decrease the inlet membrane dilution rate in this region, there is a decrease on the productivity as the conversion goes down to 0.932 just before the Hopf bifurcation appears, giving a 7.18% decrease in the effectiveness of the fermentation process. Also the ethanol yield decreases a 7.94% (decrease from $Y_P = 0.4539$–$Y_P = 0.4205$).

The stabilizing global effect of the membrane, can be summarized as follows: It destroys the static bifurcation and make it a unique state as the membrane dilution rate increases, from what was described in region one. Then the attractor becomes unstable and a periodic attractor is born (homoclinically, as described on region two). Further increase in $D_{M_{in}}$ stabilizes this periodic attractor through a Hopf bifurcation into a unique stable high conversion steady state.

Regarding the evaluation of the membrane we can be conclude that for high values of the membrane dilution rate the system is stabilized and achieves higher glucose conversion, ethanol yield and ethanol productivity steady states (Table 5).

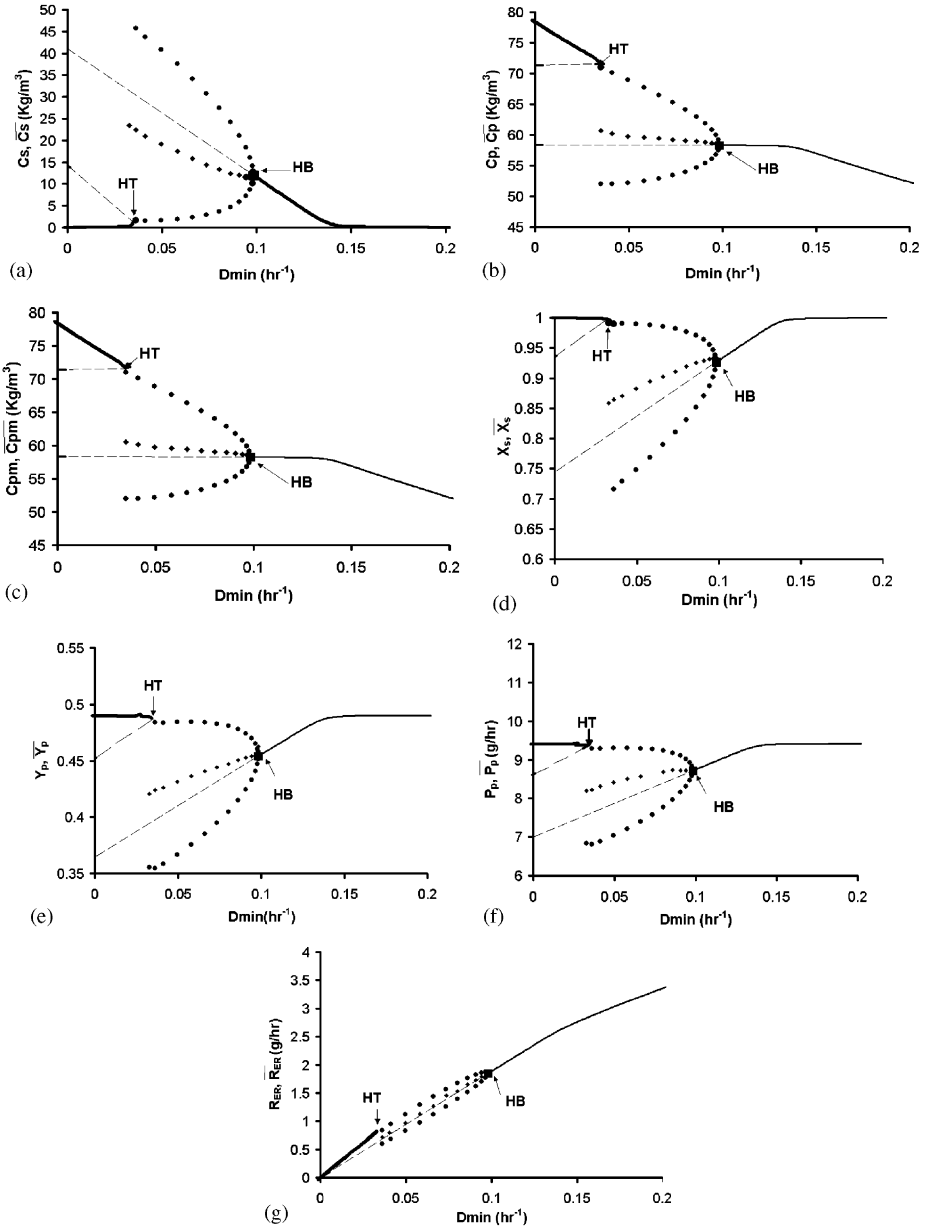

Fig. 9. Bifurcation diagrams including oscillations averages (inlet membrane dilution rate as the bifurcation parameter, $A_M = 0.24\,m^2$, $D_{in} = 0.04\,h^{-1}$, $C_{S_0} = 160\,kg/m^3$): (a) fermentor glucose concentration; (b) fermentor ethanol concentration; (c) membrane ethanol concentration; (d) glucose conversion; (e) ethanol yield; (f) ethanol production rate; (g) rate of ethanol removal. Steady state branch (stable: _____, unstable: – – – – –), periodic branch (stable: ●●●●●, average of oscillations: ♦♦♦♦♦). HB: Hopf bifurcation, HT: Homoclinical termination.

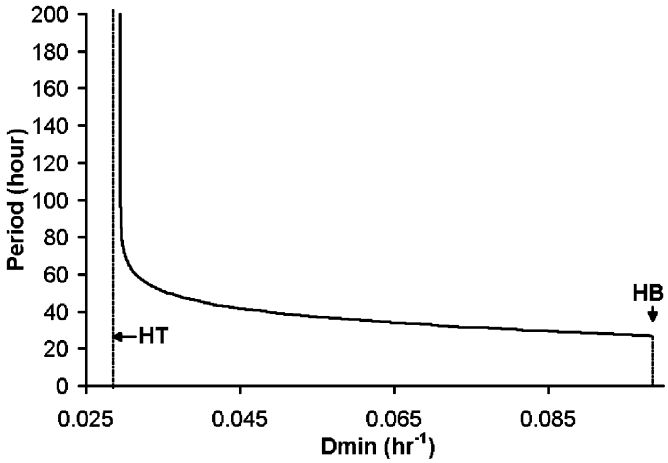

Fig. 10. Period of oscillations for the periodic branch ($A_M = 0.24\,m^2$, $D_{in} = 0.04\,h^{-1}$, $C_{S_0} = 160\,kg/m^3$). HB: Hopf bifurcation, HT: Homoclinical termination.

Table 5
Membrane improvements using high inlet membrane dilution rates

Variable (Case B.3)	Average value at $D_{M_{in}} = 0.0327$	High flow rate ($D_{M_{in}} = 0.2$)	Improvement ($D_{M_{in}} = 0.2$)
P_P (g/h)	8.2	9.4128	14.7902%
$\overline{Y_P}$	0.4205	0.4902	16.5755%
$\overline{X_S}$	0.858	0.999736	16.5193%

8. Conclusions and recommendations

The bifurcation behaviour of a continuous stirred tank fermentor with and without ethanol selective membrane has been investigated using an experimentally verified mathematical model.

In certain regions of parameters, the oscillatory behaviour in this region improves the fermentation process because the oscillation averages give higher efficiencies than their corresponding steady states (case A.1 and A.2). The inlet substrate concentration increase destabilizes the system (as it increases; a Hopf Bifurcation appears) for a non-membrane configuration (case A.2). At very high glucose concentrations those oscillations collapse and allow again a very high conversion steady state to appear. In the other hand if a high inlet membrane dilution rate is used in the membrane configuration (case A.2) all bifurcation phenomena disappears as all oscillations are avoided maintaining a constant downstream ethanol concentration. This phenomena could be very important for recovery and product quality control purposes.

The membrane dilution rate stabilizes the system (as it increases; oscillations are reduced; and eventually eliminated). Also as the flow inside the membrane is increased, the conversion increases as well as the yield and the production rate. The highest conversion, yield and productivity steady states for a set value of the inlet glucose concentration are achieved at high membrane dilution rates. This result was expected because as the inlet membrane dilution rate is increased; the ethanol removal is enhanced as well as the product inhibition is avoided. This gives rise to a higher productivity and enhances the efficiency of the process.

For an inlet glucose concentration of $140\,kg/m^3$ (case B.2) the dilution rate should be kept above $0.077\,h^{-1}$ in order to achieve conversions around 0.99. In the multiplicity region (case B.3) for an inlet glucose concentration of $160\,kg/m^3$ the dilution rate should be kept above $0.15\,h^{-1}$, this way a high efficiency steady state will be the system attractor avoiding the oscillations. Regarding the membrane dilution rate stabilizing effect for the case (B.3), we can say that its increase destroys the static bifurcation and make it a unique state. Then it creates a unique unstable steady state, and a periodic attractor is born (homoclinically). Further increase of this membrane dilution rate stabilizes this periodic attractor trough a Hopf bifurcation into a unique stable, high conversion steady state.

For all the discussed cases, the oscillations demonstrated to improve the fermentation process in the periodic attractor regions. All oscillatory attractors gave better (averaged) results for the fermentation process than the ones from their corresponding unstable steady states, this idea was discussed extensively by Al-Haddad [2] and Garhyan et al. [13] with regard to the practical exploitation of these periodic regions on the fermentation process.

The above results can be summarized in the following points:

1. The system showed static bifurcation (multiplicity of the steady state) over a wide range of parameters.
2. In the simplest cases, a *HB* point existed on one of the static branches and the periodic branch emanating from it, terminated homoclinically at an infinite period bifurcation (*HT* point) when the periodic attractor touched the saddle-type steady state in the multiplicity region.
3. Analysis of the periodic regions shows that in these regions the average sugar conversion, ethanol yield and production rate of the periodic attractors can be higher than their corresponding steady state values.
4. Using membrane fermentor, sugar conversion, ethanol yield and productivity increase as the ethanol inhibition barrier is overcome.
5. The membrane acts as a stabilizer for the fermentor thus removing the instabilities of the fermentation diffusion system, and allowing high-productivity steady states.

References

[1] F. Alfani, L. Cantarella, A. Gallifuoco, M. Cantarella, Membrane reactors for the investigation of product inhibition enzyme activity, J. Membrane Sci. 52 (1990) 339–950.

[2] S.M. Al-Haddad, Bifurcation and chaos in an experimental fermentor with Zymomonas mobilis at high ethanol concentration, M.Sc. Thesis, Salford University, Salford, UK.

[3] B. Atkinson, F. Mavituna, Biochemical Engineering and Biotechnology Handbook, second ed., Nature Press, New York, 1983.

[4] J.E. Bailey, D.F. Ollis, Biochemical Engineering Fundamentals, McGraw-Hill Chemical Engineering Series, New York, 1977.
[5] L.J. Bruce, D.B. Axford, B. Ciszek, J. Daugulis, Extractive fermentation by Zymomonas mobilis the control of oscillatory behaviour, Biotechnol. Lett. 13 (1993) 291–296.
[6] A.J. Daugulis, D.B. Axford, B. Ciszek, J.J. Malinowski, Continuous fermentation of high-strength glucose feeds to ethanol, Biotechnol. Lett. 16 (1994) 637–641.
[7] E.J. Doedel, A.R. Champneys, T.F. Fairgrieve, Y.A. Sandstede, X.J. Wang, AUTO97: Continuation and Bifurcation Software for Ordinary Differential Equations, Department of Computer Science, Concordia University, Montreal, Canada.
[8] M. Elly, M.B. Cutlip, M. Shacham, Polymath 5.0, University of Connecticut, Ben Gurion University of Negev and The University of Michigan, 2000.
[9] S.S.E.H. Elnashaie, A.H. Fakeeha, E. Helal, E. Abashar, A mathematical model achieving the twin objectives of simplicity and accuracy for the simulation of immobilized packed bed fermentors, Math. Comput. Model. 19 (1994) 105–114.
[10] B. Ermentrout, XPPAUT5.0- The Differential Equations Tool, 2001.
[11] R.L. Fournier, Mathematical model of microporous hollow-fiber membrane extractive fermentor, Biotechnol. Bioeng. 31 (1988) 235–239.
[12] P. Garhyan, S.S.E.H. Elnashaie, Utilization of mathematical models to investigate the bifurcation and chaotic behavior of ethanol fermentors, Math. Comput. Model. 39 (2004) 381–427.
[13] P. Garhyan, S.S.E.H. Elnashaie, S.M. Al-Haddad, G. Ibrahim, S.S. Elshishini, Exploration and exploitation of bifurcation/chaotic behavior of a continuous fermentor for the production of ethanol, Chem. Eng. Sci. 58 (2003) 1479–1496.
[14] C. Ghommidh, J. Vaija, S. Bolarinwa, J.M. Navarro, Oscillatory behaviour of Zymomonas mobilis in continuous cultures: a simple stochastic model, Biotechnol. Lett. 2 (1989) 659–664.
[15] W.D. Hsieh, R.H. Chen, T.L. Wu, T.H. Lin, Engine performance and pollutant emission of an SI engine using ethanol-gasoline blended fuels, Atmos. Environ. 36 (2002) 403–410.
[16] A.B. Jarzebski, Modeling of oscillatory behaviour in continuous ethanol fermentation, Biotechnol. Lett. 14 (1992) 137–142.
[17] Y.S. Jeong, W.R. Vieth, T. Matsuura, Transport and kinetics in sandwiched membrane bioreactors, Biotechnol. Prog. 7 (1991) 130–139.
[18] I.M.L. Jobses, Modeling of anaerobic microbial fermentations: the production of alcohols by Zymomonas mobilis and Clostridium beijerincki, Ph.D. Thesis, Delft University, Delft, Holland, 1986.
[19] I.M.L. Jobses, G.T.C. Egberts, A.V. Ballen, J.A. Roels, Mathematical modeling of growth and substrate conversion of Zymomonas mobilis at 30 and 35 °C, Biotechnol. Bioeng. 27 (1985) 984–995.
[20] I.M.L. Jobses, G.T.C. Egberts, K.C.A.M. Luyben, J.A. Roels, Fermentation kinetics of Zymomonas mobilis at high ethanol concentrations: oscillations in continuous cultures, Biotechnol. Bioeng. 28 (1986) 868–877.
[21] J.P. Keener, Infinite period bifurcation and global bifurcation branches, J. Appl. Math. 41 (1981) 127–144.
[22] K.T. Knapp, F.D. Stump, S.B. Tejada, The effect of ethanol fuel on the emissions of vehicles over a wide range of temperatures, J. Air Waste Manage. Assoc. 48 (1998) 646–653.
[23] M. Kralik, V. Macho, N. Brautbar, A. Vachalkova, J. Mikulec, Engine fuels in the 21st century, Petroleum Coal 43 (2001) 72–79.
[24] P.J. McLellan, A.J. Daugulis, J. Li, The incidence of oscillatory behaviour in the continuous fermentation of Zymomonas mobilis, Biotechnol. Prog. 15 (1999) 667–680.
[25] S.F. Naser, R.L. Fournier, A numerical evaluation of a hollow fiber extractive fermentor process for the production of ethanol, Biotechnol. Bioeng. 32 (1988) 628–638.
[26] J.H. Perry, Chemical Engineer's Handbook, Chemical Engineering Series, McGraw Hill, New York, 1973.
[27] S.J. Pirt, The maintenance energy of bacteria in growing cultures, Proc. Roy. Soc. Lond. Ser. B: Biol. Sci. 163 (1965) 224–231.
[28] O.P. Ward, A. Singh, Bioethanol technology: developments and perspectives, Adv. Appl. Microbiol. 51 (2002) 53–80.
[29] S. Wolfram, The Mathematica Book, Wolfram Media/C.U.P., Cambridge, 1999.
[30] C.E. Wyman, Ethanol from lignocellulosic biomass: technology, economics, and opportunities, Bioresour. Technol. 50 (1994) 3–15.